Biogeosciences Discuss., https://doi.org/10.5194/bg-2017-507
Manuscript under review for journal Biogeosciences
Discussion started: 18 December 2017

Physical and chemical evolution of dissolved organic matter across the ablation season on a glacier in the central Tibetan Plateau

Lin Feng[1,3], YanqingAn[1], JianzhongXu[1*], Shichang Kang[1,2,3], Xiaofei Li[1,2], Yongqiang Zhou[4], Yunlin Zhang[4], Bin Jiang[5],Yuhong Liao[5]

[1]State Key Laboratory of Cryospheric Sciences, Northwest Institute of Eco-Environment and Resources, Chinese Academy of Sciences, Lanzhou 730000, China, [2]CAS Center for Excellence in Tibetan Plateau Earth Sciences , [3]University of Chinese Academy of Sciences, Beijing 100049, China, CAS Center for Excellence in Tibetan Plateau Earth Sciences,[4]State Key Laboratory of Lake Science and Environment, Nanjing Institute of Geography and Limnology, Chinese Academy of Sciences,73 East Beijing Road, Nanjing 210008, China, [5]State Key Laboratory of Organic Geochemistry, Guangzhou Institute of Geochemistry, Chinese Academy of Sciences, Wushan, Guangzhou 510640, PR China

Corresponding author email: jzxu@lzb.ac.cn

Biogeosciences Discuss., https://doi.org/10.5194/bg-2017-507
Manuscript under review for journal Biogeosciences
Discussion started: 18 December 2017

Abstract

The physical evolution (metamorphism) of snow is known to affect the chemical composition of dissolved organic matter (DOM) within it. Here, we present a comprehensive study on the Dongkemadi glacier in the central Tibetan Plateau by analyzing surface snow/ice samples collected from May to October 2015. Based on their physical descriptions, these samples were grouped into four categories, i.e., fresh snow, fine firn, coarse firn, and granular ice that represented the different stages of snowmelt. The concentrations of dissolved organic carbon (DOC) decreased from fresh snow (26.8 μmol L^{-1}) to fine firn (15.0 μmol L^{-1}), then increased from fine firn to coarse firn (26.1 μmol L^{-1}) and granular ice (34.4 μmol L^{-1}). This reflected the dynamic variations in DOC observed during snowmelt. The use of excitation emission matrix fluorescence with parallel factor analysis (EEM-PARAFAC) identified three protein-like components (C1, C2 and C4) and one microbial humic-like component (C3), which reflected the presence of significant amounts of microbially derived DOM in surface snow/ice. The molecular level compositions of DOM identified using Fourier transform ion cyclotron resonance mass spectrometry (FT-ICR-MS) also showed the presence of molecules that were newly produced during snowmelt. These results suggest that snowmelt not only induced a loss of DOM but also intensified the *in situ* microbial activities that enriched and modified it. These findings are important for understanding the evolution of the physical and chemical characteristics of DOM during the ablation season and can also shed some light on the nature of biogeochemical cycles in cryospheric regions.

Biogeosciences Discuss., https://doi.org/10.5194/bg-2017-507
Manuscript under review for journal Biogeosciences
Discussion started: 18 December 2017

1. Introduction

Mountain glaciers are a critical source of fresh water, and their response to climate change can have an impact on the regional water supply. In addition to playing a role in the hydrological cycle, glacier melt water also exerts an important influence on the biogeochemical properties of downstream ecosystems, such as glacial lakes and rivers (Robinson et al., 2016;Singer et al., 2012;Saros et al., 2010). For example, high concentrations of mineral suspensoids in glacial melt water cause the water in glacier-fed lakes to be highly turbid, which leads to unfavorable conditions for primary producers, such as planktonic taxa (Sommaruga, 2015). In contrast with their physical roles, the chemical functions of glacial streams may be even more important because they can directly influence downstream ecosystems by providing nutrients for biomes. Hood et al. (2009) observed that the high bioavailability of dissolved organic matter (DOM) in glacial streams had a high impact on marine microorganisms in the coastal zone. Additionally, significantly increased chlorophyll levels have been observed around icebergs during the melting of giant icebergs (Duprat et al., 2016), which suggests that the DOM in icebergs can influence microbial activities and can have a further impact on the net primary productivity in the ocean (Wu and Hou, 2017). Due to the high abundances and large degree of chemical diversity of DOM in global glacial streams (e.g., C, N, P, and S) (Fegel et al., 2016;Hood et al., 2015;Singer et al., 2012), the biogeochemical effects of glacial melt water have recently attracted much attention.

The Tibetan Plateau (TP) is referred to as the “Water Tower of Asia”, as it is the source of the ten largest rivers in Asia, which feed more than 1 billion people. For example, glacial melt water accounted for 14.6% − 61.11% of the water resources in the rivers of Western China between 1957 and 2005 (Zhang et al., 2010a). Meanwhile, glacier ablation is one of most important

Biogeosciences Discuss., https://doi.org/10.5194/bg-2017-507
Manuscript under review for journal Biogeosciences
Discussion started: 18 December 2017

factors controlling the chemical characteristics of the headwaters of the major Asian rivers in the TP (Xiang et al., 2009). Recently, Xu et al. (2013) found that contributions of DOM could account for more than 50% of the dissolved substances in samples collected from glaciers in the Himalayas. Liu et al. (2016) estimated the storage and annual release rates of dissolved organic carbon (DOC) in mountain glaciers in Western China and found that they were more efficient to be released than those observed in the Polar Regions. However, the overall qualities of DOM and its associated reactivity, which is related to its chemical composition and molecular characteristics, remain poorly characterized.

Our previous work on the chemical composition of cryoconite (which is a dark-colored, dust-like material found on the surfaces of glaciers) in the ablation areas of glaciers revealed the presence of saturated organic matter, such as lipids and proteins, which could have been generated by *in situ* microbial activities (Feng et al., 2016). Spencer et al. (2014) estimated the bioavailability of this saturated organic matter and found that it reached values of up to ~50%. However, the dynamic evolution of chemical components from fresh snow to ice during the ablation process is less well characterized.

During ablation, glaciers can undergo leaching effects, in which certain amounts of soluble matter, such as water-soluble inorganic ions, are lost (Hou and Qin, 1999). However, few studies have analyzed the leaching effects of DOM during the process of melting. Voisin et al. (2012) showed the evolution of DOC using various types of snow samples based on their physical processes in Arctic snowpack. The variability of DOM during ablation could not only cause their mass concentrations to decrease but could also cause their chemical compositions to evolve due to *in situ* chemical processes (Grannas et al., 2014). For example, microbially reworked DOM in supraglacial deposits exhibits an increase in the number and magnitude of its N-, S-, and P-

Biogeosciences Discuss., https://doi.org/10.5194/bg-2017-507
Manuscript under review for journal Biogeosciences
Discussion started: 18 December 2017

containing formulas, which are less oxygenated and more aromatic than the initial DOM (Antony et al., 2017).

Therefore, the goals of this paper are to (1) examine the compositions and sources of DOM in snow samples collected from the Dongkemadi (DKMD) glacier in the TP and (2) evaluate the dynamic nature of the DOM and its molecular compounds observed during snowmelt.

2. Experimental Details

2.1 Sites and Sampling

This field campaign was carried out on the DKMD glacier in the Tanggula Mountain region, which is located in the central part of the TP, from May 2015 to October 2015. The glacier is a typical valley glacier with a length of 2.8 km and an area of 1.767 km^2. The elevations of the summit and the terminus of the glacier are 5926 and 5380 m a.s.l., respectively. Due to the rapid increase in air temperature that has occurred in recent decades, this glacier has experienced severe ablation (Pu et al., 2008). According to data obtained from the automatic meteorological station, which is located near the equilibrium line (5600 m a.s.l.) on the glacier, its annual precipitation is approximately 300 mm and is dominated by summer precipitation from the Asian monsoon. Surface snow/ice samples were collected along the glacier (at a depth of ~10 cm) from the lower to higher elevation areas at intervals of ~50 m. At each elevation, two to five parallel samples were collected from the left, middle, and right sides of the glacier (Figure 1). Sample collection was carried out once every month from May 2015 to October 2015, and a total of ~36 samples were collected during each collection period. Samples were collected using a stainless steel scoop, which could easily collect aged snow and ice; they were then placed in acid-cleaned Teflon bottles. All samples were melted at room temperature and passed through 0.45-μm filters

Biogeosciences Discuss., https://doi.org/10.5194/bg-2017-507
Manuscript under review for journal Biogeosciences
Discussion started: 18 December 2017

at base camp before being transported to the lab. The samples were kept frozen during transportation using a cooler box and blue ice.

A total of 178 snow/ice samples were processed in this study. These samples were grouped into four different types of snow/ice samples based on their physical characteristics, i.e., fresh snow, fine firn, coarse firn, and granular ice, which represent the different stages of snowmelt, from beginning to end, respectively. The numbers of samples in each category and their distribution on the glacier during each month are shown in Figure S1. Almost all fresh snow and fine firn samples were collected in May, with fine firn samples located at lower elevations and fresh snow samples located at higher elevations. Most of the coarse firn samples were collected in June and July and were widely distributed over the surface of the glacier, as they were formed from fresh snow under the influence of increased air temperature. Most of the granular ice samples were collected in September and October and were formed by further freeze-thaw processes taking place on coarse snow. A total of 14 samples comprising mixtures of fresh snow and coarse firn were collected in August, and this type of sample was eliminated from our discussion due to the mixed signals that were obtained during snowmelt.

2.2 DOC Analysis

Filtered snow/ice samples were melted at room temperature in their capped bottles prior to undergoing further chemical analysis. A 10-mL aliquot of each melted snow/ice sample was acidified with 100 μL of 10% hydrochloric acid in order to remove inorganic carbonates; they were then passed through a Vario EL CN analyzer (Elementar, Hanau, Germany). Non-purgeable organic carbon was then oxidized by combusting the sample at 850 ℃ in a carrier gas with a controlled O_2 concentration; the evolved gases that contained carbon were converted to

Biogeosciences Discuss., https://doi.org/10.5194/bg-2017-507
Manuscript under review for journal Biogeosciences
Discussion started: 18 December 2017

CO_2, which was then measured using a non-dispersive infrared analyzer. The system was calibrated using a potassium hydrogen phthalate standard.

2.3 Absorption measurements

The light absorbances of all melted samples were determined using a UV-visible absorption spectrophotometer (UV-2410PC, Shimadzu, Japan) with a 1-cm quartz cuvette within a spectrum of 200-900 nm at 1-nm increments. Blanks of Milli-Q water were used as references. Absorbance spectra were baseline-corrected by subtracting the mean absorbance for the spectral range from 690 nm to 700 nm. Optical density values (i.e., absorbance values) were converted to absorption coefficients by fitting the equation:

$$a(\lambda) = 2.303 \cdot \mathrm{A}(\lambda)/\mathrm{L} \qquad (1)$$

where $\mathrm{A}(\lambda)$ is the measured absorbance for a wavelength λ, L is the path length of the optical cell (here, L = 0.01 m), and 2.303 is the common-to-natural logarithm conversion factor.

The DOM spectral slope (S) was obtained from a nonlinear fit over the 240-400 nm wavelength range using the following equation:

$$a(\lambda) = a(\lambda_0)e^{S(\lambda_0-\lambda)} + \mathrm{k} \qquad (2)$$

Where $a(\lambda)$ and $a(\lambda_0)$ are the absorption coefficients at wavelengths of λ and 300 nm, respectively; and S and k are the spectral slope and the estimated background parameter, respectively.

Note that the sample absorption coefficient $a(\lambda)$ at a given wavelength represents the sum of the absorption coefficient contributions from all chromophores, including DOM and nitrate, at that wavelength. To eliminate the interference of nitrate on the absorption properties of DOM, we estimated the absorption coefficient of the optical absorption of nitrate. The absorption

Biogeosciences Discuss., https://doi.org/10.5194/bg-2017-507
Manuscript under review for journal Biogeosciences
Discussion started: 18 December 2017

coefficient of nitrate at each wavelength, $a(NO_3^-, \lambda)$, was determined for each snow sample using the following equation:

$$a(NO_3^-, \lambda) = \varepsilon(NO_3^-, \lambda) \cdot [NO_3^-] \quad (3)$$

Where $\varepsilon(NO_3^-, \lambda)$ is the molar absorptivity of NO_3^- at λ and $[NO_3^-]$ is the molar concentration of NO_3^- in the melted snow sample. We adopted the $\varepsilon(NO_3^-, \lambda)$ values (220-350 nm) measured in the lab in a previous study (Beine et al., 2011), and the values of $[NO_3^-]$ used here were measured using ion chromatography in our lab.

The average specific UV absorbance at 254 nm (SUVA254), which is an indicator of the aromaticity and chemical reactivity of DOM, was calculated by dividing the average absorptivity at λ=254 nm by the average concentration of DOC, in units of L mg $C^{-1}M^{-1}$ (Weishaar et al., 2003).

2.4 Three-dimensional fluorescence measurements

All fluorescence spectra measurements were made using a HitachiF-7000 fluorescence spectrometer (Hitachi High-Technologies, Tokyo, Japan) with a 700-voltage xenon lamp following the method of Zhang et al. (2010b). The excitation wavelength (Ex) ranged from 200 to 450 nm, using an interval of 5 nm, while the emission wavelength (Em) ranged from 250 to 600 nm, using an interval of 2 nm. Both the Ex and the Em slit widths were set at 5 nm. The scan speed was 2400 nm min^{-1}.

The Raman scatter of the water was calibrated by subtracting the daily excitation emission matrix (EEM) fluorescence values of the Milli-Q water blanks (Zhou et al., 2015). The Rayleigh scatter effects were eliminated by excluding any emission measurements made at wavelengths that were ≤ excitation wavelength + 15 nm, or at wavelengths that were ≥ 2 × excitation wavelength - 20 nm, followed by replacing the values in the two triangular regions of the EEMs

Biogeosciences Discuss., https://doi.org/10.5194/bg-2017-507
Manuscript under review for journal Biogeosciences
Discussion started: 18 December 2017

with zeros (Zhang et al., 2010b;Zhou et al., 2015). To correct for inner filter effects, the approach described by Zhou et al. (2015) was applied, in which absorbance measurements were made using a 4-cm quartz cuvette on a Shimadzu UV-2450PC spectrophotometer with Milli-Q water as a reference. To remove instrument-dependent intensity effects, we present our results on a unified scale of Raman units following the method of Lawaetz and Stedmon (2009). Unreliable instrument measurements were eliminated by deleting excitation wavelengths of 200-225 nm and emission wavelengths between 250-299 and 550-600 nm (Zhou et al., 2016).

2.5 PARAFAC modeling

PARAFAC statistically decomposes complex mixtures of DOM fluorophores into individual components without making any assumptions about their spectral shapes or their number. The combination of EEMs and PARAFAC has been widely applied to characterize DOM in aquatic environments and in glacier research (Barker et al., 2009). Each component identified using PARAFAC has a unique excitation and emission spectrum, and each component may comprise a single fluorophore or a group of similar fluorophores. PARAFAC separates the data signal into a set of three linear terms and a residual array.

In this study, this analysis was carried out using MATLAB 12a with PARAFAC using the drEEM toolbox (ver. 0.2.0), according to the method proposed by Murphy et al. (2013). The dataset used for PARAFAC modeling was composed of 127 snow/ice samples and an EEM matrix of excitation wavelengths ranging from 230 to 450 nm and emission wavelengths ranging from 300 to 550 nm. The results were decomposed into a four-component result that explained more than 97.8% of the EEM variables.

A series of optical parameters, including the fluorescence index (FI), biological index (BIX), and humification index (HIX), were obtained from the EEMs. The FI is calculated as the ratio of the

Biogeosciences Discuss., https://doi.org/10.5194/bg-2017-507
Manuscript under review for journal Biogeosciences
Discussion started: 18 December 2017

emission intensity at 470 nm to that at 520 nm, both of which are obtained from excitation at 370 nm (Cory and McKnight, 2005). A value of FI of 1.4 or less indicates that the DOM is of terrestrial origin; a value of FI of 1.9 or higher indicates that the DOM represents microbe-derived material (Birdwell and Engel, 2010). The BIX is calculated as the ratio of the emission intensities at 380 and 430 nm, both of which are obtained from excitation at 310 nm (Fellman et al., 2010). Values of BIX falling in the range of 0.8−1.0 are characteristic of freshly produced DOM of biological or microbial origin, whereas values below ~0.6 indicate that little autochthonous organic matter is present (Birdwell and Engel, 2010). A modified HIX is calculated using the area under an emission spectrum (acquired using excitation at 254 nm) between 435 and 480 nm and dividing it by the area under the spectrum between 300 and 345 nm plus the area under the spectrum between 435 and 480 nm; these values were used to compare the humification levels of different DOM samples (Birdwell and Engel, 2010).

2.6 ESI-FT-ICR-MS Analysis

Four samples with different snow/ice physical characteristics were analyzed using ESI-FT-ICR-MS. Prior to this analysis, these samples were prepared using PPL (Agilent Bond Elut-PPL cartridges, 500 mg, 6 mL) solid phase extraction (SPE) cartridges to concentrate the DOM and remove inorganic salts. The details of the SPE method using PPL cartridges were described in our previous study (Feng et al., 2016). Briefly, the prepacked PPL cartridges were first conditioned with approximately 20 mL of LC-MS grade methanoland3 column volumes of acidified ultrapure water (pH =2, LC-MS grade HCl). Approximately 150 mL of each sample was acidified to a pH of 2 (using 0.1 M LC-MS grade HCl) and extracted through the PPL cartridges with a flow rate of less than 1 mL/min. After undergoing extraction, the cartridges were dried and then eluted with ~10 mL of methanol. Eluted samples were blow-dried with N_2 to

Biogeosciences Discuss., https://doi.org/10.5194/bg-2017-507
Manuscript under review for journal Biogeosciences
Discussion started: 18 December 2017

~1 mL and were then immediately stored in a freezer (4 ℃). A procedural blank using Milli-Q water was also obtained following the procedure described above to determine if any potential contamination occurred during the sample preprocessing.

The mass spectrometry analyses of these samples were performed using a SolariX XR FT-ICR-MS (Bruker Daltonik GmbH, Bremen, Germany) equipped with a 9.4 T refrigerated actively shielded superconducting magnet (Bruker Biospin, Wissembourg, France) and a Paracell analyzer cell. The samples were ionized in both negative and positive ion modes using the ESI ion source (Bruker Daltonik GmbH, Bremen, Germany). Ions were accumulated in the hexapole for 1 s before being transferred to the ICR cell. The mass detection range was set to m/z 150 – 800. A 4 M word size was selected for the time domain signal acquisition. A total of 100 continuous FI-ICR transients were accumulated to enhance the signal-to-noise ratio and the dynamic range. The procedural blanks were processed and analyzed following the same procedure to detect any possible contamination. A typical mass-resolving power (m/Δm50%, in which Δm50% is the magnitude of the full width of the mass spectral peak at its half-maximum peak height) of >400 000 was achieved at m/z 400 with an absolute mass error of <0.5 ppm.

2.7 Molecular Formula Assignment

Molecular formulas were assigned to all ions with signal-to-noise ratios of greater than 10 with a mass tolerance of ±1.5 ppm using custom software. We only analyzed the data obtained in positive mode because the data obtained in negative mode were disturbed by Cl^-. Molecular formulas with their maximum numbers of atoms were defined as: 30 ^{12}C, 60 ^{1}H, 20 ^{16}O, 3 ^{14}N, 1 ^{32}S, 1 ^{13}C, 1 ^{18}O and 1 ^{34}S. Identified formulas containing isotopomers (i.e., ^{13}C, ^{18}O or ^{34}S) were not considered. For the chemical formula $C_cH_hO_oN_nS_s$, the DBE was calculated using the

Biogeosciences Discuss., https://doi.org/10.5194/bg-2017-507
Manuscript under review for journal Biogeosciences
Discussion started: 18 December 2017

following equation: DBE = (2*c*+2-*h*+*n*)/2. The details of this data processing method have previously been described (Jiang et al., 2014;Quan et al., 2013).

To identify the biomolecular class to which each molecular compound belonged, a van Krevelen diagram was used, in which elemental H/C ratios were plotted against elemental O/C ratios. Here, we follow the protocols that have been proposed by many authors (Grannas et al., 2006;Hockaday et al., 2009;Ide et al., 2017). Each molecular compound was divided into seven biomolecular classes based on a series of ranges of O/C and H/C values. The seven classes are defined as (1) lipids ($0 \leq O/C < 0.3$, $1.5 < H/C < 2.4$), (2) proteins ($0.3 \leq O/C \leq 0.67$, $1.5 < H/C < 2.4$), (3) carbohydrates/amino sugars ($0.67 < O/C < 1.2$, $1.5 < H/C < 2.4$), (4) unsaturated hydrocarbons ($0 < O/C < 0.1$, $0.7 \leq H/C \leq 1.5$), (5) lignins/CRAM ($0.1 \leq O/C \leq 0.67$, $0.7 \leq H/C \leq 1.5$), (6) tannins ($0.67 < O/C < 1.2$, $0.5 \leq H/C \leq 1.5$), and (7) condensed aromatics ($0 < O/C \leq 0.67$, $0.2 \leq H/C < 0.7$).

3. RESULTS

3.1 DOC Concentrations and UV-Visible Absorbance of Snow/Ice Samples

The DOC concentrations of each sample along with their elevations are shown in Supporting Information Figure S1. The DOC concentrations of these samples ranged in 1.1 – 189 μmol L^{-1}; their monthly mean values are presented in Figure 2a, in which their maximum values were observed in September (59.6 μmol L^{-1}), followed by August (35.7 μmol L^{-1}), October (26.4 μmol L^{-1}), May (22.8 μmol L^{-1}), June (19.8 μmol L^{-1}), and July (18.6 μmol L^{-1}). The median values of the DOC concentrations measured in each month followed the same trend (not shown). The variations in the chemical contents of the snow/ice samples are consistent with the variations in their UV-Vis absorbance spectra (Figure 2b). The sum of the absorbance between 190-500 nm in each monthly average spectrum varied evidently; the maximum value of 896 was measured in

Biogeosciences Discuss., https://doi.org/10.5194/bg-2017-507
Manuscript under review for journal Biogeosciences
Discussion started: 18 December 2017

September, followed by May (887), October (731), August (462), June (450) and July (444). The average absorbance spectra observed during each month exhibited significant absorbance between 190–250 nm; however, the samples collected during September and October also showed some absorbance between 250–400 nm, thus suggesting that different chemical compositions were present during these months.

The average DOC concentration of fresh snow was 26.8 μmol L^{-1}, which decreased to 15 μmol L^{-1} for fine firn; these concentrations then gradually increased for coarse firn (26.2 μmol L^{-1}) and granular ice (34.4 μmol L^{-1}) (Figure 3a). The standard deviations of the DOC mass concentrations in each snow category were less than those observed in the monthly average snow samples (±16.9 μmol L^{-1} vs. ±17.7 μmol L^{-1}) (Figure 3a). In addition, the median values of the DOC concentrations for each category were 25.4 μmol L^{-1} for fresh snow, 16 μmol L^{-1} for fine firn, 24 μmol L^{-1} for coarse firn and 24.6 μmol L^{-1} for granular ice.

The average absorption coefficient of each category of samples was high for short wavelengths and decreased sharply above 240 nm (Figure 3b). The total absorption coefficient of each category showed obvious differences in its characteristics between 240–400 nm, between which the granular ice samples showed their most significant peak. Considering the potential light absorption of nitrate, we estimated the contributions of nitrate based on its measured concentrations using a laboratory-generated standard absorption spectrum (Beine et al., 2011). The average contribution of nitrate to the total absorbance in each category was less than 10%; therefore, we only show an average spectrum of nitrate in Figure 3b. The SUVA254 values obtained for each sample category were 4.41 for fresh snow, 4.36 for fine firn, 4.01 for coarse firn, and 4.91 for granular ice; these values suggest that there are relatively high abundances of aromatic components in this component. The values of the spectral slope between 240–400 nm

Biogeosciences Discuss., https://doi.org/10.5194/bg-2017-507
Manuscript under review for journal Biogeosciences
Discussion started: 18 December 2017

($S_{240\text{-}400}$) for each category were 26.3 μm^{-1} for fresh snow, 25.4 μm^{-1} for fine firn, 16.44 μm^{-1} for coarse firn, and 12.55 μm^{-1} for granular ice, which suggests that the molecular weight of the DOM increased during each melting stage (Murphy et al., 2006).

3.2 Fluorescent DOM components

The spectral characteristics of each of the identified components are shown as functions of their excitation and emission wavelengths and fluorescence intensity, which are expressed in QSU units, in Figure 4. The four identified components include three protein-like components (C1, C2 and C4) and a humic-like component (C3) (Table 1). The fluorescent loading patterns of the four modeled components can be matched to fluorophores described by other authors (Table S1), as is described in the Supporting Information section.

The relative contributions of C1 and C2 account for an average value of approximately 80% of the total DOM fluorescence in each category of samples (Figure 5), which suggests that they record an important microbial origin. The relative abundance of C1 decreased with increasing degrees of snow melt, as it gradually decreased from 44% in fine firn to 35% in granular ice; in contrast, the relative abundances of C2 and C3 increased from 38% in fine firn to 44% in granular ice and from 12% in fresh snow to 14% in granular ice, respectively (Figure 5).

3.3 FT-ICR-MS Analysis of DOM Compositions in Each Snow Category

The van Krevelen diagrams (H:C vs O:C) constructed for each category of samples revealed a high degree of molecular diversity in terms of their DOM compositions, ranging from fresh snow to granular ice (Figure 6). The assigned molecular compounds are mainly concentrated in three biomolecular classes, i.e., lipids (29.2% – 42%), proteins (33% – 40.3%), and lignins (19% – 27%). Different chemical classes in each category of samples exhibited clear trends (Table 3). The relative contributions of proteins and lignins generally increased from 33% to 40.3% and

Biogeosciences Discuss., https://doi.org/10.5194/bg-2017-507
Manuscript under review for journal Biogeosciences
Discussion started: 18 December 2017

from 19% to 27%, respectively, from fine firn to granular ice. The relative contributions of lipids (from 42% to 29.2%), unsaturated hydrocarbon content (from 3% to 1.7%), and condensed aromatics (from 1% to 0.5%) all exhibited decreasing trends (Table 3). Notably, the fractions of protein and lignin classes in fresh snow were higher than those in fine firn. In addition, differences in the chemical compositions of DOM were observed in different categories of samples. The average molecular mass of the assigned DOM gradually increased from fine firn (376) to granular ice (396) (Table 3), and the assigned molecular number increased from 2469 to 3933 (Table 4). The relative mass content of carbon (C_m) in each average formula of the molecular classes decreased in lipids, unsaturated hydrocarbons, and condensed aromatics, thus reflecting the chemical process of the addition of other elements in these components (Table S2). The van Krevelen plots were also colored based on the presence of different molecular classes, i.e., CHO, CHN, and CHON (Figure 6). The contributions of these classes in the four categories of snow samples are shown in Table 4. We found that the contributions of CHO molecules decreased from 77.3% to 71.7% from fine firn to granular ice, while those of CHON molecules increased from 22.2% to 28.2%. Therefore, the ratio between CHON and CHO increased significantly, from 0.287 to 0.393, from fine firn to granular ice. We also calculated the percentages of molecules with low C/N ratios (≤20) in each category of samples; these values increased from 10 to 17.7% from fresh snow to granular ice.

We further analyzed the effects of snow melting on DOM compositions by directly comparing the unique and overlapping assigned molecular compounds in the four snow categories of samples using a simple Venn diagram (Figure 7). Most (1836) of the identified molecular components in these four categories overlapped, thus indicating that this DOM has a high degree of similarity. However, granular ice exhibits the most unique molecular components (461),

Biogeosciences Discuss., https://doi.org/10.5194/bg-2017-507
Manuscript under review for journal Biogeosciences
Discussion started: 18 December 2017

followed by coarse firn (225), fine firn (163) and fresh snow (153), which suggests that the process of snowmelt significantly alters the composition of DOM.

4. DISCUSSION

4.1 The effect of snow melting on the chemical content of DOM in snow/ice

The concentrations of DOC in snow/ice could be related to their chemical compositions during their original deposition as well as to post-depositional processes, which could have redistributed and modified their chemical compositions and mass concentration. The monthly average DOC concentrations during summer (June, July, and August) were all at the low range of their values, suggesting that the snowmelt could have lost DOC. In contrast, most of the samples collected during May comprised fresh snow that had not yet melted, with no loss or modification of their chemical contents, such that their concentrations were higher than those observed during June and July. Quantitatively, DOC concentrations decreased from 26.8 μmol L^{-1} in the fresh snow samples to 15 μmol L^{-1} in the fine firn samples. This indicates that approximately 44% of the compounds were lost during the first stage of snowmelt. Measurements of DOC performed in the stream at the end of the DKMD indicated that the mass concentrations of DOC observed during June and July were higher than observed in other months (unpublished data). This phenomenon was also observed for some organic contaminants in snowpack in a remote alpine area, in which their concentrations were also high in early melt water (Lafrenière et al., 2006). Grannas et al. (2013) summarized the elution behavior of snowpack for different types of contaminants; Water-soluble species are released quickly in early melt water, which can be explained by the percolation of melt water flowing down from the snowpack, which dissolves the ions excluded from the ice matrix that are present within a liquid-like layer at the snow-grain surface.

Biogeosciences Discuss., https://doi.org/10.5194/bg-2017-507
Manuscript under review for journal Biogeosciences
Discussion started: 18 December 2017

From fine firn to granular ice samples, the DOC increased from 15 μmol L^{-1} to 34.4 μmol L^{-1}, respectively, suggesting that the enrichment of DOM occurred during snowmelt. The process of snowmelt is dominated by repeated melting and freezing processes which can cause the coarsening of the snow grain (Wakahama, 1968). In addition, due to the erosion of debris that occurs on the mountain around the glacier caused by melted snowpack, a certain amount of mineral dust can be transported to the surface of the glacier during the melt season. The enrichment of mineral nutrients and aqueous conditions on the surface of the glacier represent favorable conditions for the growth of biota, which could originate from an Aeolian biome. Cryoconite granules, comprising both mineral and biological material, could thus eventually form. These processes from the beginning of snow melt to form of cryoconite granules can last for more than 5 months in the TP. However, the enrichment or reduction of DOM in cryoconite is balanced by the production and consumption of DOM from microbial activities. Bagshaw et al. (2016) suggested that DOM in cryoconite is consumed (i.e., net heterotrophy) during the first few days, while DOM is produced (i.e., net autotrophy) after a period of approximately 20-40 days. The chemical content produced from cryoconite is diversity and significant, and many studies have focused on the potential biogeochemical effects of microbial metabolism due to the production of nutrients during this process (Bagshaw et al., 2016;Feng et al., 2016;Fountain et al., 2004;MacDonell et al., 2016).

4.2 The chemical composition, sources, and evolution of DOM in snow/ice

The EEM results showed that the DOM was generally dominated by protein-like (C1, C2 and C4) and humic-like components (C3). The relative abundance of the three protein-like components (C1, C2 and C4) accounted for more than 85% of the total DOM fluorescence in each category of samples, while the humic-like component accounted for the remaining 15% (Figure 6). This

Biogeosciences Discuss., https://doi.org/10.5194/bg-2017-507
Manuscript under review for journal Biogeosciences
Discussion started: 18 December 2017

finding is consistent with that of another study, which recorded relatively low ratios of humic- to protein-like fluorescence in different types of snow/ice samples from seven glaciers in the Canadian Arctic, Norway, and Antarctica (Dubnick et al., 2010). The high contribution of protein-like material in the snow/ice samples indicates the important contribution of microbially derived DOM. This conclusion is also supported by their lower HIX (0.27–0.37) and higher BIX (0.71–0.8) values (Table 2), which differ from those found in samples from Lake Taihu (in which the values of HIX ranged from 0.47 to 2.19 and those of BIX ranged from 0.83-1.15) (Zhou et al., 2015) and even differ from those of cryoconite samples from the same glacier (in which the values of HIX ranged from 1.11 to 1.37 and those of BIX ranged from 0.65 to 0.93) (Feng et al., 2016), thus indicating the relatively fresh nature of DOM in snow/ice samples. The results of FT-ICR-MS analysis further showed that the predominance of microbial products (including lipids and proteins) contributed to more than half of the identified molecular species (Table 4). A small fraction of terrestrial components, including tannins and lignins/CRAM molecules, was also observed. Other studies that have used FT-ICR-MS reported similar DOM components from surface snow and glaciers in the Antarctic (Antony et al., 2014), and Greenland (Bhatia et al., 2010). More intense microbial signals were observed in snow/ice compared with that in cryoconite samples (Table 3).

In addition to the *in-situ* production of DOM, a mixture of terrestrial and microbially derived organic material may be expected from an array of different sources, such as suspended soil and dust particles, biogenic emissions, and organic substances generated by atmospheric processes. Mixed chemical compositions were found not only in granular ice samples but also in fresh snow samples, which were mainly composed of atmospheric aerosols from within and outside of clouds. These mixed chemical characteristics were also seen in other studies of fog water (Zhao

Biogeosciences Discuss., https://doi.org/10.5194/bg-2017-507
Manuscript under review for journal Biogeosciences
Discussion started: 18 December 2017

et al., 2013) and ambient aerosols (Mazzoleni et al., 2012) in other remote areas. This suggests that the aerosols in this remote area of the TP mostly originated from natural sources. Numerous studies have suggested that primary biological aerosol particles (PBAPs), including bacteria, spores and pollen, may be important for atmospheric processes, including those involved in the formation of clouds and precipitation (Despréś et al., 2012). Biological aerosols could be more abundant during summer due to more favorable air temperature and humidity conditions (Toprak and Schnaiter, 2013), which could be the source of the microbially derived components (including lipids and proteins) in fresh snow. Secondary organic aerosols, which are produced by the oxidation of volatile organic compounds emitted from biogenic and anthropogenic sources, are thought to be important in aerosol compositions, especially in remote areas. However, the chemical compositions of our fresh snow samples did not appear to show this characteristic. One possible reason for this is that secondary organic aerosols are commonly observed in fine particles (less than 1 μm in diameter), while PBAPs are found in coarser particles (1 – 20 μm) (Huffman et al., 2010), which dominant the mass fraction.

Although protein-like material was dominant in all samples, the chemical compositions of the granular ice were also different than those of fresh snow. The fact that the absorbance observed at 250 – 500 nm was higher in granular ice than it was in fresh snow reflects the higher aromaticity of the DOM. The variation in the $S_{240\text{-}400}$ values of DOM gradually decreased from fresh snow to granular ice, thus implying that the molecular weight of the DOM increased during the snowmelt process. These results suggest the presence of microbially transformed and newly produced DOM in the glacier samples by other chemical processes (Mcneill et al., 2012). A diverse assemblage of bacteria, archaea, and eukarya in the snow pack could produce one or more enzymes (including lipase, protease, amylase, β-galactosidase, cellulase, and lignin-

Biogeosciences Discuss., https://doi.org/10.5194/bg-2017-507
Manuscript under review for journal Biogeosciences
Discussion started: 18 December 2017

modifying enzyme) that could utilize the DOM (Antony et al., 2016) and produce microbially derived organic material, i.e., by microbial metabolism. The higher contributions from tyrosine-like (Figure 4) and nitrogen-containing compounds in granular ice recorded compared with fresh snow (Table 4) suggest microbial production. The relatively higher abundances of the molecules gradually changing from high DBE- to zero DBE-containing molecules during snowmelt, accompanied by increased oxygen content (Figure 8), suggests the occurrence of oxidation process.

5. Conclusions

The DOC concentrations of snow/ice samples in the DKMD glacier ranged in 1.1 – 189 μmol L^{-1}, and their monthly mean values reached a maximum in September (59.6 μmol L^{-1}) and a minimum in July (18.6 μmol L^{-1}). The average value for fresh snow was 26.8 μmol L^{-1}, which decreased to 15 μmol L^{-1} for fine firn and gradually increased for coarse firn (26.2 μmol L^{-1}) and granular ice (34.4 μmol L^{-1}). This suggests that the percolation from fresh snow to fine firn on the glacier results in the significant loss of DOM (~44%), while the DOM is dramatically enriched (~129%) from fine firn to granular ice. The EEMs, combined with PARAFAC modeling, revealed three protein-like components (C1, C2 and C4) and one humic-like component (C3). The FT-ICR-MS results showed that the molecular composition of the DOM mainly included lipids (29.2% – 42%), proteins (33% –40.3%), and lignins (19% – 27%). The relative abundance of C1 gradually decreased with increasing degrees of snow melt, from 44% (fine firn) to 35% (granular ice), while the relative abundances of C2 and C3 showed increasing trends, increasing from 38% (fine firn) to 44% (granular ice) and from 12% (fresh snow) to 14% (granular ice), respectively. The relative contributions of proteins and lignins generally increased from 33% to 40.3% and from 19% to 27%, respectively, from fine firn to granular ice. While the

Biogeosciences Discuss., https://doi.org/10.5194/bg-2017-507
Manuscript under review for journal Biogeosciences
Discussion started: 18 December 2017

relative contributions of lipids (from 42% to 29.2%), unsaturated hydrocarbon content (from 3% to 1.7%), and condensed aromatics (from 1% to 0.5%) all exhibited decreasing trends. These results thus provide strong evidence for the microbial source of the DOM on the surface of the TP glacier during snowmelt. Consequently, against the background of global warming, the DOM released from the glacier will feed the downstream ecosystem, where it will also likely have increased biogeochemical effects.

Acknowledgments

This research was supported by grants from the Key Laboratory of Cryospheric Sciences Scientific Research Foundation (SKLCS-ZZ-2017), the National Natural Science Foundation of China (41330526), the National Natural Science Foundation of China Science Fund for Creative Research Groups (41421061), and the Chinese Academy of Sciences Hundred Talents Program. The data used here are listed in tables and in the Supporting Information section.

Biogeosciences Discuss., https://doi.org/10.5194/bg-2017-507
Manuscript under review for journal Biogeosciences
Discussion started: 18 December 2017

References

Antony, R., Grannas, A. M., Willoughby, A. S., Sleighter, R. L., Thamban, M., and Hatcher, P. G.: Origin and Sources of Dissolved Organic Matter in Snow on the East Antarctic Ice Sheet, Environ. Sci. Technol., 48, 6151–6159, 2014.

Antony, R., Sanyal, A., Kapse, N., Dhakephalkar, P. K., Thamban, M., and Nair, S.: Microbial communities associated with Antarctic snow pack and their biogeochemical implications, Microbiol. Res., 192, 192–202, 2016.

Antony, R., Willoughby, A. S., Grannas, A. M., Catanzano, V., Sleighter, R. L., Thamban, M., Hatcher, P. G., and Nair, S.: Molecular Insights on Dissolved Organic Matter Transformation by Supraglacial Microbial Communities, Environ. Sci. Technol., 51, 4328–4337, 2017.

Bagshaw, E. A., Wadham, J. L., Tranter, M., Perkins, R., Morgan, A., Williamson, C. J., Fountain, A. G., Fitzsimons, S., and Dubnick, A.: Response of Antarctic cryoconite microbial communities to light, FEMS Microbiol. Ecol., 92, fiw076, 2016.

Barker, J. D., Sharp, M. J., and Turner, R. J.: Using synchronous fluorescence spectroscopy and principal components analysis to monitor dissolved organic matter dynamics in a glacier system, Hydrol. Processes, 23, 1487–1500, 2009.

Beine, H., Anastasio, C., Esposito, G., Patten, K., Wilkening, E., Domine, F., Voisin, D., Barret, M., Houdier, S., and Hall, S.: Soluble, light‐absorbing species in snow at Barrow, Alaska, J. Geophys. Res.: Atmos., 116, 2011.

Bhatia, M. P., Das, S. B., Longnecker, K., Charette, M. A., and Kujawinski, E. B.: Molecular characterization of dissolved organic matter associated with the Greenland ice sheet, Geochim. Cosmochim. Acta, 74, 3768–3784, 2010.

Birdwell, J. E., and Engel, A. S.: Characterization of dissolved organic matter in cave and spring waters using UV-Vis absorbance and fluorescence spectroscopy, Org. Geochem., 41, 270–280, 2010.

Cory, R. M., and McKnight, D. M.: Fluorescence Spectroscopy Reveals Ubiquitous Presence of Oxidized and Reduced Quinones in Dissolved Organic Matter, Environ. Sci. Technol., 39, 8142–8149, 2005.

Despréś, V. R., Huffman, J. A., Burrows, S. M., Hoose, C., Safatov, A. S., Buryak, G., Fröhlich-Nowoisky, J., Elbert, W., Andreae, M. O., and Pöschl, U.: Primary biological aerosols in the atmosphere: A review Tellus B, 64, 15598, 2012.

Dubnick, A., Barker, J., Sharp, M., Wadham, J., Lis, G., Telling, J., Fitzsimons, S., and Jackson, M.: Characterization of dissolved organic matter (DOM) from glacial environments using total fluorescence spectroscopy and parallel factor analysis, Ann. Glaciol., 51, 111–122, 2010.

Duprat, L. P. A. M., Bigg, G. R., and Wilton, D. J.: Enhanced Southern Ocean marine productivity due to fertilization by giant icebergs, Nat. Geosci., 9, 219–221, 2016.

Fegel, T. S., Baron, J. S., Fountain, A. G., Johnson, G. F., and Hall, E. K.: The Differing Biogeochemical and Microbial Signatures of Glaciers and Rock Glaciers, J. Geophys. Res.: Biogeosci., 121, 919–932, 2016.

Fellman, J. B., Hood, E., and Spencer, R. G. M.: Fluorescence spectroscopy opens new windows into dissolved organic matter dynamics in freshwater ecosystems: a review, Limnol. Oceanogr., 55, 2452–2462, 2010.

Feng, L., Xu, J., Kang, S., Li, X., Yang, L., Jiang, B., and Quan, S.: Chemical Composition of Microbe-Derived Dissolved Organic Matter in Cryoconite in Tibetan Plateau Glaciers: Insights from Fourier Transform Ion Cyclotron Resonance Mass Spectrometry Analysis, Environ. Sci. Technol., 50, 13215–13223, 2016.

Fountain, A. G., Tranter, M., Nylen, T. H., Lewis, K. J., and Mueller, D. R.: Evolution of cryoconite holes and their contribution to meltwater runoff from glaciers in the McMurdo Dry Valleys, Antarctica, J. Glaciol., 50, 35–45, 2004.

Grannas, A., C. Bogdal, K. Hageman, C. Halsall, T. Harner, H. Hung, R. Kallenborn, P. Klán, J. Klánová, and Macdonald, R.: The role of the global cryosphere in the fate of organic contaminants, Atmos. Chem. Phys., 13, 3271–3305, 2013.

Grannas, A. M., Hockaday, W. C., Hatcher, P. G., Thompson, L. G., and Ellen, M. T.: New revelations on the nature of organic matter in ice cores, J. Geophys. Res.: Atmos., 111, 2006.

Grannas, A. M., Pagano, L. P., Pierce, B. C., Bobby, R., and Fede, A.: Role of Dissolved Organic Matter in Ice Photochemistry, Environ. Sci. Technol., 48, 10725–10733, 2014.

Hockaday, W. C., Purcell, J. M., Marshall, A. G., Baldock, J. A., and Hatcher, P. G.: Electrospray and photoionization mass spectrometry for the characterization of organic matter in natural waters: a qualitative assessment, Limnol. Oceanogr.: Methods, 7, 81–95, 2009.

Hood, E., J, F., RG, S., PJ, H., R, E., D, D. A., and D, S.: Glaciers as a source of ancient and labile organic matter to the marine environment, Nature, 462, 1044–1047, 2009.

Hood, E., Battin, T. J., Fellman, J., O'Neel, S., and Spencer, R. G. M.: Storage and release of organic carbon from glaciers and ice sheets, Nat. Geosci., 8, 91–96, 2015.

Hou, S. G., and Qin, D. H.: The Ion Elution Effect on the Main Ion Profiles of the Glacier Snowpacks, Scientia Geographica Sinica, 19, 536–542, 1999.

Huffman, J. A., Treutlein, B., and Schl, U. P.: Fluorescent biological aerosol particle concentrations and size distributions measured with an Ultraviolet Aerodynamic Particle Sizer (UV-APS) in Central Europe, Atmos. Chem. Phys., 10, 3215–3233, 2010.

Ide, J., Ohashi, M., Takahashi, K., Sugiyama, Y., Piirainen, S., Kortelainen, P., Fujitake, N., Yamase, K., Ohte, N., and Moritani, M.: Spatial variations in the molecular diversity of dissolved organic matter in water moving through a boreal forest in eastern Finland, Sci. Rep., 7, 2017.

Jiang, B., Liang, Y., Xu, C., Zhang, J., Hu, M., and Shi, Q.: Polycyclic aromatic hydrocarbons (PAHs) in ambient aerosols from Beijing: characterization of low volatile PAHs by positive-ion atmospheric pressure photoionization (APPI) coupled with Fourier transform ion cyclotron resonance, Environ. Sci. Technol., 48, 4716–4723, 2014.

Lafrenière, M. J., J. M. Blais, M. J. Sharp, and Schindler, D. W.: Organochlorine Pesticide and Polychlorinated Biphenyl Concentrations in Snow, Snowmelt, and Runoff at Bow Lake, Alberta, Environ. Sci. Technol., 40, 4909–4915, 2006.

Lawaetz, A. J., and Stedmon, C. A.: Fluorescence intensity calibration using the Raman scatter peak of water, Appl. Spectrosc., 63, 936–940, 2009.

Liu, Y., Jianzhong, X. U., Kang, S., Xiaofei, L. I., and Yang, L. I.: Storage of dissolved organic carbon in Chinese glaciers, J. Glaciol., 62, 402–406, 2016.

MacDonell, S., M. Sharp, and Fitzsimons, S.: Cryoconite hole connectivity on the Wright Lower Glacier, McMurdo Dry Valleys, Antarctica, J. Glaciol., 62, 714–724, 2016.

Mazzoleni, L. R., Saranjampour, P., Dalbec, M. M., Samburova, V., Hallar, A. G., Zielinska, B., Lowenthal, D. H., and Kohl, S.: Identification of water-soluble organic carbon in non-urban

aerosols using ultrahigh-resolution FT-ICR mass spectrometry: Organic anions, Environ. Chem., 9, 285–297, 2012.

Mcneill, V. F., Grannas, A. M., Abbatt, J. P. D., Ammann, M., Ariya, P., Bartelsrausch, T., Domine, F., Donaldson, D. J., Guzman, M. I., and Heger, D.: Organics in environmental ices: sources, chemistry, and impacts, Atmos. Chem. Phys., 12, 9653–9678, 2012.

Murphy, K. R., Ruiz, G. M., Dunsmuir, W. T., and Waite, T. D.: Optimized parameters for fluorescence-based verification of ballast water exchange by ships, Environ. Sci. Technol., 40, 2357–2362, 2006.

Murphy, K. R., Stedmon, C. A., Graeber, D., and Bro, R.: Fluorescence spectroscopy and multi-way techniques. PARAFAC, Anal. Methods, 5, 6557–6566, 2013.

Pu, J., Yao, T., Yang, M., Tian, L., Wang, N., Ageta, Y., and Fujita, K.: Rapid decrease of mass balance observed in the Xiao (Lesser) Dongkemadi Glacier, in the central Tibetan Plateau, Hydrol.Processes, 22, 2953–2958, 2008.

Quan, S., Na, P., Long, H., Cui, D., Guo, X., Long, Y., Chung, K. H., Zhao, S., Xu, C., and Chang, S. H.: Characterization of Middle-Temperature Gasification Coal Tar. Part 3: Molecular Composition of Acidic Compounds, Energy Fuels, 27, 108–117, 2013.

Robinson, C. T., Tonolla, D., Imhof, B., Vukelic, R., and Uehlinger, U.: Flow intermittency, physico-chemistry and function of headwater streams in an Alpine glacial catchment, Aquat. Sci., 78, 327–341, 2016.

Saros, J. E., Rose, K. C., Clow, D. W., Stephens, V. C., Nurse, A. B., Arnett, H. A., Stone, J. R., Williamson, C. E., and Wolfe, A. P.: Melting Alpine glaciers enrich high-elevation lakes with reactive nitrogen, Environ. Sci. Technol., 44, 4891–4896, 2010.

Singer, G. A., Fasching, C., Wilhelm, L., Niggemann, J., Steier, P., Dittmar, T., and Battin, T. J.: Biogeochemically diverse organic matter in Alpine glaciers and its downstream fate, Nat. Geosci., 5, 710–714, 2012.

Sommaruga, R.: When glaciers and ice sheets melt: consequences for planktonic organisms, J. Plankton Res.,, 37, 509–518, 2015.

Spencer, R. G. M., Guo, W., Raymond, P. A., Dittmar, T., Hood, E., Fellman, J., and Stubbins, A.: Source and biolability of ancient dissolved organic matter in glacier and lake ecosystems on the Tibetan Plateau, Geochim. Cosmochim. Acta, 142, 64–74, 2014.

Toprak, E., and Schnaiter, M.: Fluorescent biological aerosol particles measured with the Waveband Integrated Bioaerosol Sensor WIBS-4: laboratory tests combined with a one year field study, Atmos. Chem. Phys., 13, 225–243, 2013.

Voisin, D., Jaffrezo, J. L., Houdier, S., Barret, M., Cozic, J., King, M. D., France, J. L., Reay, H. J., Grannas, A., and Kos, G.: Carbonaceous species and humic like substances (HULIS) in Arctic snowpack during OASIS field campaign in Barrow, J. Geophys. Res.: Atmos., 117, 2012.

Wakahama, G.: The metamorphism of wet snow, IAHS Publ., 1968.

Weishaar, J. L., Aiken, G. R., Bergamaschi, B. A., Fram, M. S., Fujii, R., and Mopper, K.: Evaluation of specific ultraviolet absorbance as an indicator of the chemical composition and reactivity of dissolved organic carbon, Environ. Sci. Technol., 37, 4702–4708, 2003.

Wu, S. Y., and Hou, S.: Impact of icebergs on net primary productivity in the Southern Ocean, The Cryosphere, 11, 1-13, 2017.

Xiang, H., Sillanpää, M., Gjessing, E. T., and Vogt, R. D.: Water quality in the Tibetan Plateau: Major ions and trace elements in the headwaters of four major Asian rivers, Sci. Total Environ., 407, 6242–6254, 2009.

Biogeosciences Discuss., https://doi.org/10.5194/bg-2017-507
Manuscript under review for journal Biogeosciences
Discussion started: 18 December 2017

Xu, J., Zhang, Q., Li, X., Ge, X., Xiao, C., Ren, J., and Qin, D.: Dissolved organic matter and inorganic ions in a central Himalayan glacier--insights into chemical composition and atmospheric sources, Environ. Sci. Technol., 47, 6181–6188, 2013.

Zhang, Q., Xu, C. Y., Tao, H., Jiang, T., and Chen, Y. D.: Climate changes and their impacts on water resources in the arid regions: a case study of the Tarim River basin, China, Stochastic Environmental Research & Risk Assessment, 24, 349–358, 2010a.

Zhang, Y., Zhang, E., Yin, Y., Dijk, M. A. V., Feng, L., Shi, Z., Liu, M., and Qina, B.: Characteristics and sources of chromophoric dissolved organic matter in lakes of the Yungui Plateau, China, differing in trophic state and altitude, Limnol. Oceanogr., 55, 2645–2659, 2010b.

Zhao, Y., Hallar, A. G., and Mazzoleni, L. R.: Atmospheric organic matter in clouds: exact masses and molecular formula identification using ultrahigh resolution FT-ICR mass spectrometry, Atmos. Chem. Phys., 13, 12343–12362, 2013.

Zhou, Y., Zhang, Y., Shi, K., Niu, C., Liu, X., and Duan, H.: Lake Taihu, a large, shallow and eutrophic aquatic ecosystem in China serves as a sink for chromophoric dissolved organic matter, J. Great Lakes Res., 41, 597–606, 2015.

Zhou, Y., Zhou, J., Jeppesen, E., Zhang, Y., Qin, B., Shi, K., Tang, X., and Han, X.: Will enhanced turbulence in inland waters result in elevated production of autochthonous dissolved organic matter?, Sci. Total Environ., 543, 405–415, 2016.

Biogeosciences Discuss., https://doi.org/10.5194/bg-2017-507
Manuscript under review for journal Biogeosciences
Discussion started: 18 December 2017

Tables and Figures

Table 1. Description of the four-component PARAFAC model. Wavelengths in parentheses represent secondary peaks.

Component number	Excitation maxima nm	Emission maxima nm	Description
C1	<230 285	322	Protein-like (tryosine-like or tyrosine-like), Peak T or Peak B
C2	270	308	Protein-like (tyrosine-like), Peak B
C3	<230	424	Humic-like, Peak M
C4	240 290	340	Protein-like (tryptophan-like), Peak T

Biogeosciences Discuss., https://doi.org/10.5194/bg-2017-507
Manuscript under review for journal Biogeosciences
Discussion started: 18 December 2017

Table 2. Fluorescence Indices (FIs), Humification Indices (HIXs), and Biological Indices (BIXs) for DOMs extracted from the snow/ice samples in this study and from cryoconite samples in the TGL [*Feng et al.*, 2016].

Sample type	FI	HIX	BIX
Surface snow samples			
Fresh snow	2.47 ±0.32	0.27 ±0.04	0.71±0.08
Fine firn	2.15 ±0.38	0.31 ±0.12	0.8 ±0.12
Coarse firn	2.14 ±0.32	0.3 ±0.16	0.77 ±0.15
Granular ice	2.02 ±0.25	0.37 ±0.24	0.74 ±0.19
Cryoconite samples			
TGL2	3.17	1.32	0.65
TGL3	3.12	1.11	0.93

Biogeosciences Discuss., https://doi.org/10.5194/bg-2017-507
Manuscript under review for journal Biogeosciences
Discussion started: 18 December 2017

Table 3. Average m/z, number and distribution of van Krevelen chemical classes from the FT-ICR-MS analyses of the dissolved organic matter (DOM) components of the fresh snow, fine firn, coarse firn, granular ice and cryoconite samples [*Feng et al.*, 2016].

Sampling site	Mean mass	lipids (%)	protein (%)	carbohydrates (%)	unsaturated hydrocarbons (%)	lignins and tannins (%)	condensed aromatics (%)
Fresh snow	391	921 (31.3%)	1147(39%)	44 (1.5%)	52 (1.8%)	760 (25.8%)	19 (0.6%)
Fine firn	376	1034 (42%)	821 (33%)	41 (2%)	70 (3%)	477 (19%)	26 (1%)
Coarse firn	392	1116 (32%)	1371 (39.1%)	29 (0.8%)	78 (2.2%)	890 (25.4%)	18 (0.5%)
Granular ice	396	1147 (29.2%)	1586 (40.3%)	55 (1.4%)	67 (1.7%)	1061 (27%)	17 (0.4%)
TGL2	417	470 (31.5%)	418 (28%)	76 (5.1%)	140 (9.4%)	358 (24%)	31 (2%)
TGL3	400	378 (28%)	370 (27.4%)	67 (4.9%)	129 (9.5%)	362 (26.8%)	46 (3.4%)

Biogeosciences Discuss., https://doi.org/10.5194/bg-2017-507
Manuscript under review for journal Biogeosciences
Discussion started: 18 December 2017

Table 4. Dissolved organic carbon (DOC) and number and percentage of elemental formulas assigned to the CHO, CHON, and CHN groups in snow/ice sample and cryoconite samples [*Feng et al.*, 2016].

Sample type	DOC (μmol/L)	Total	CHO (%)	CHN (%)	CHON (%)	C/N≤20 (%)	CHON:CHO
Fresh snow	26.8 ±10.8	2943	2224 (75.5%)	0 (0%)	721 (24.5%)	295 (10%)	0.324
Fine firn	15 ±6	2469	1909 (77.3%)	13(0.5%)	547 (22.2%)	359 (14.5%)	0.287
Coarse firn	26.1 ±16	3502	2538 (72.4%)	5 (0.2%)	959 (27.4%)	570 (16.3%)	0.378
Granular ice	34.4 ±34.9	3933	2820 (71.7%)	4 (0.1%)	1109 (28.2%)	696 (17.7%)	0.393
TGL2	2.71×10^3	1493	880 (59%)	41(2.7%)	572 (38.3%)	365 (24.4%)	0.65
TGL3	3.29×10^3	1352	858 (63.4%)	59(4.4%)	435 (32.2%)	343 (25.4%)	0.507

Biogeosciences Discuss., https://doi.org/10.5194/bg-2017-507
Manuscript under review for journal Biogeosciences
Discussion started: 18 December 2017

Figure 1. Map showing the locations of glaciers in the Tibetan Plateau and the distribution of snow/ice samples collected on the Dongkemadi (DKMD) glacier.

Figure 2. (a) Average mass concentrations and (b) UV-Vis absorbance spectra of dissolved organic carbon (DOC) in snow/ice samples from each month.

Figure 3. (a) Average mass concentrations and (b) UV-Vis absorbance spectra of dissolved organic carbon (DOC) in each category of snow/ice sample.

Figure 4. Excitation-emission matrices (EEMs) for the four-component PARAFAC model.

Figure 5. The average relative contributions of the four components identified by the PARAFAC model for all fresh snow samples, fine firn samples, coarse firn samples and granular ice samples.

Figure 6. Van Krevelen diagrams for the mass spectra of samples of (a) fresh snow, (b) fine firn, (c)coarse firn, and (d) granular ice. The regions in the plots indicate the different classes of biomolecular compounds. The size of the marker indicates the relative intensity of each peak.

Figure 7. Four-way Venn diagram showing the overlap in molecular formulas between the fresh snow, fine firn, coarse firn and granular ice. The numbers within the diagram are the numbers of m/z molecular formulas that are unique to each type of sample.

Figure 8. Iso-abundance plots of DBE versus carbon numbers for all DOM components, colored according to the number content of oxygen for (a) fresh snow, (b) fine firn, (c) coarse firn, and (d) granular ice.

Biogeosciences Discuss., https://doi.org/10.5194/bg-2017-507
Manuscript under review for journal Biogeosciences
Discussion started: 18 December 2017

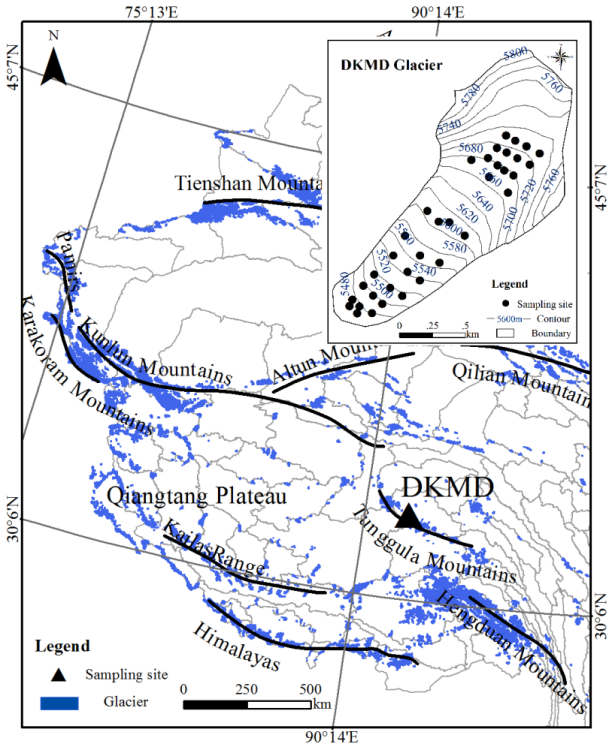

Figure 1. Map showing the locations of glaciers in the Tibetan Plateau and the distribution of snow/ice samples collected on the Dongkemadi (DKMD) glacier.

Biogeosciences Discuss., https://doi.org/10.5194/bg-2017-507
Manuscript under review for journal Biogeosciences
Discussion started: 18 December 2017

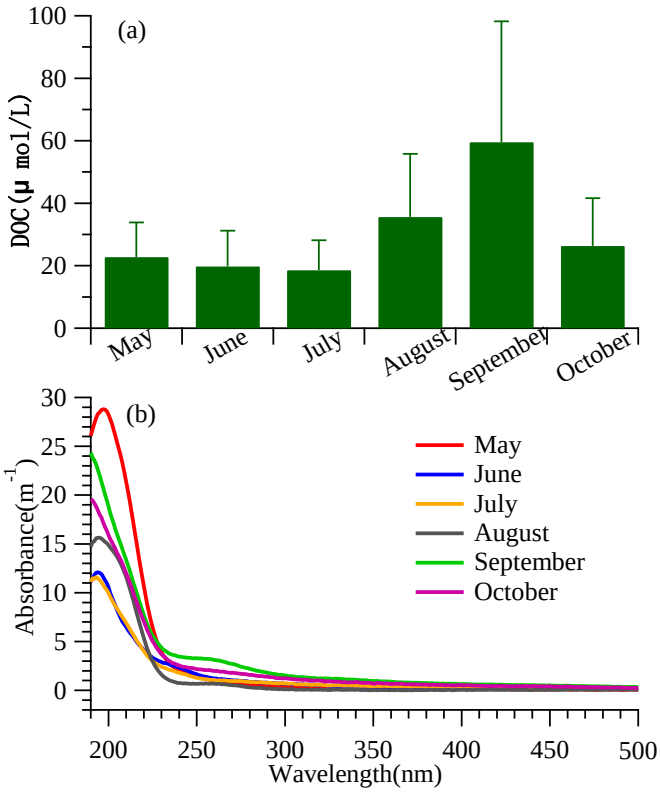

Figure 2. (a) Average mass concentrations and (b) UV-Vis absorbance spectra of dissolved organic carbon (DOC) in snow/ice samples from each month.

Biogeosciences Discuss., https://doi.org/10.5194/bg-2017-507
Manuscript under review for journal Biogeosciences
Discussion started: 18 December 2017

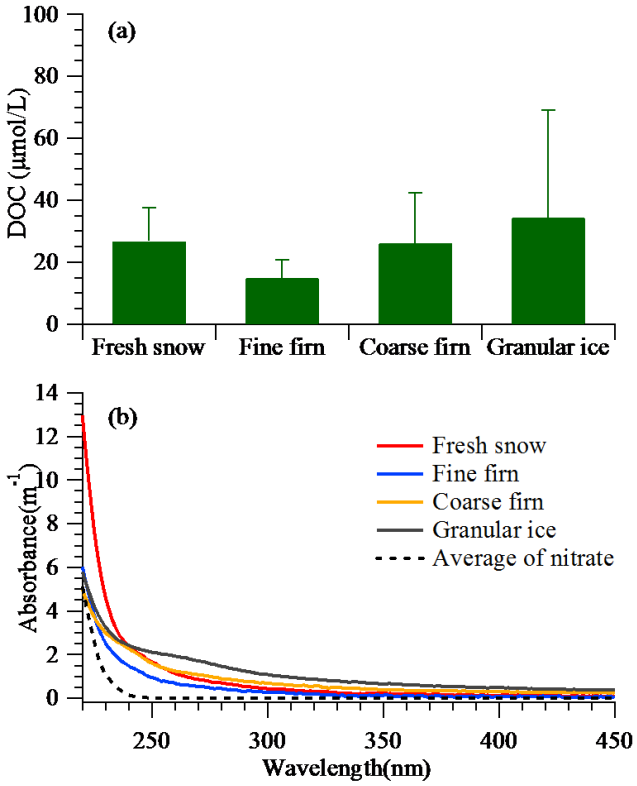

Figure 3. (a) Average mass concentrations and (b) UV-Vis absorbance spectra of dissolved organic carbon (DOC) in each category of snow/ice sample.

Biogeosciences Discuss., https://doi.org/10.5194/bg-2017-507
Manuscript under review for journal Biogeosciences
Discussion started: 18 December 2017

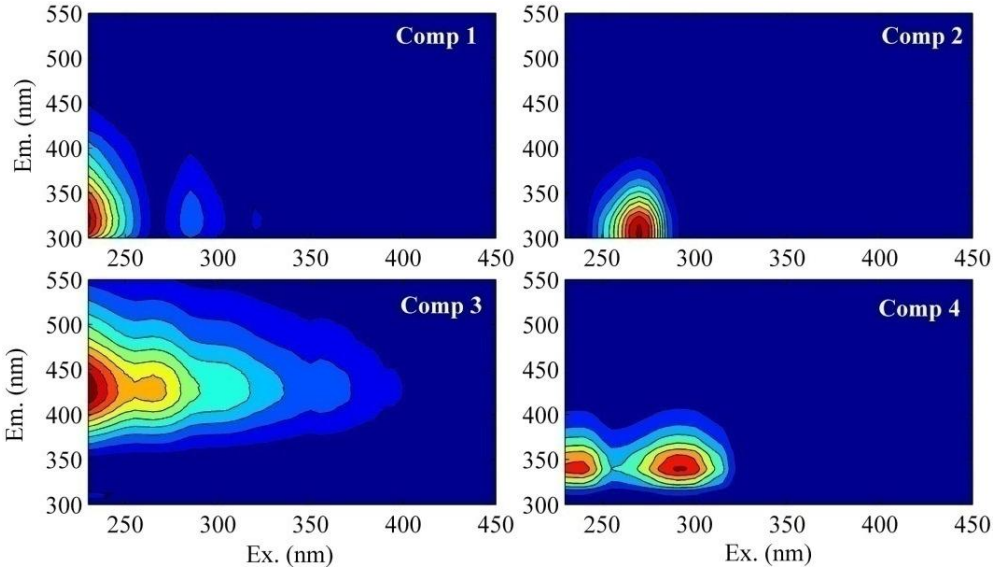

Figure 4. Excitation-emission matrices (EEMs) for the four-component PARAFAC model.

Biogeosciences Discuss., https://doi.org/10.5194/bg-2017-507
Manuscript under review for journal Biogeosciences
Discussion started: 18 December 2017

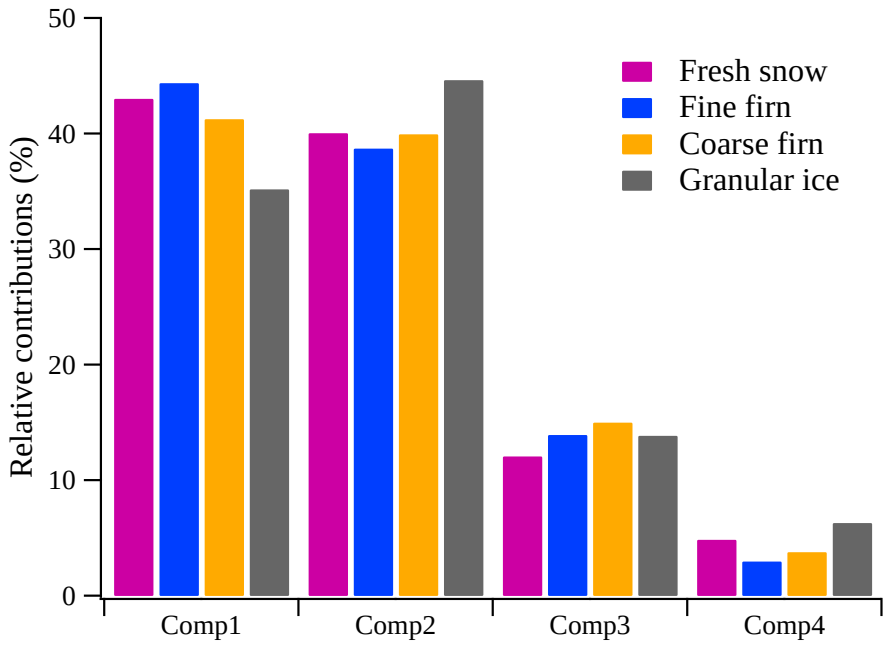

Figure 5. The average relative contributions of the four components identified by the PARAFAC model for all fresh snow samples, fine firn samples, coarse firn samples and granular ice samples.

Biogeosciences Discuss., https://doi.org/10.5194/bg-2017-507
Manuscript under review for journal Biogeosciences
Discussion started: 18 December 2017

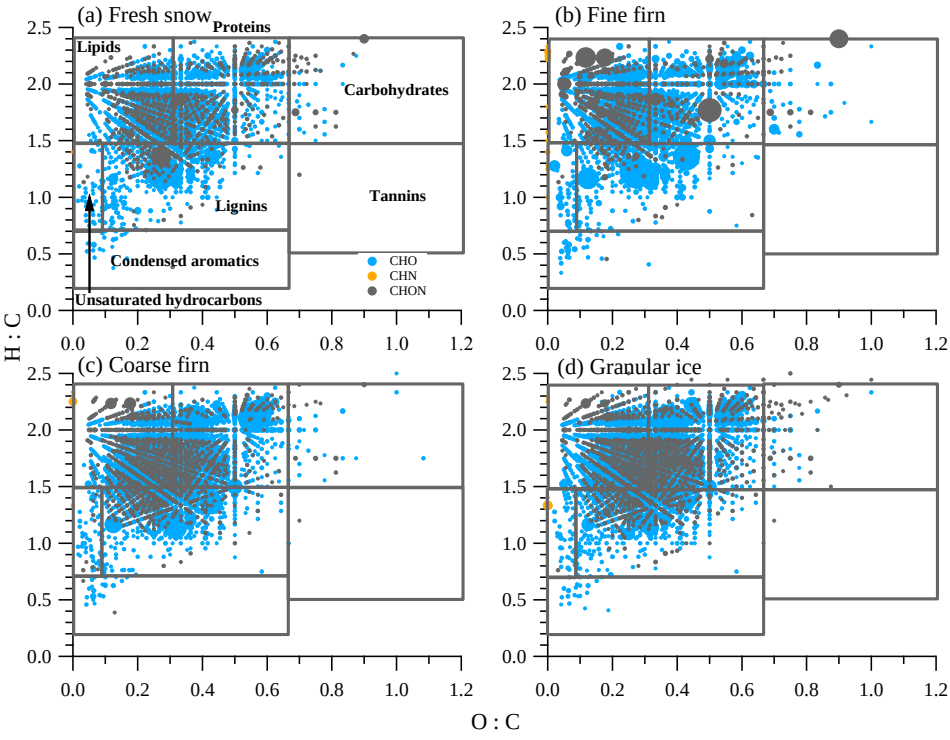

Figure 6. Van Krevelen diagrams for the mass spectra of samples of (a) fresh snow, (b) fine firn, (c) coarse firn, and (d) granular ice. The regions in the plots indicate the different classes of biomolecular compounds. The size of the marker indicates the relative intensity of each peak.

Biogeosciences Discuss., https://doi.org/10.5194/bg-2017-507
Manuscript under review for journal Biogeosciences
Discussion started: 18 December 2017

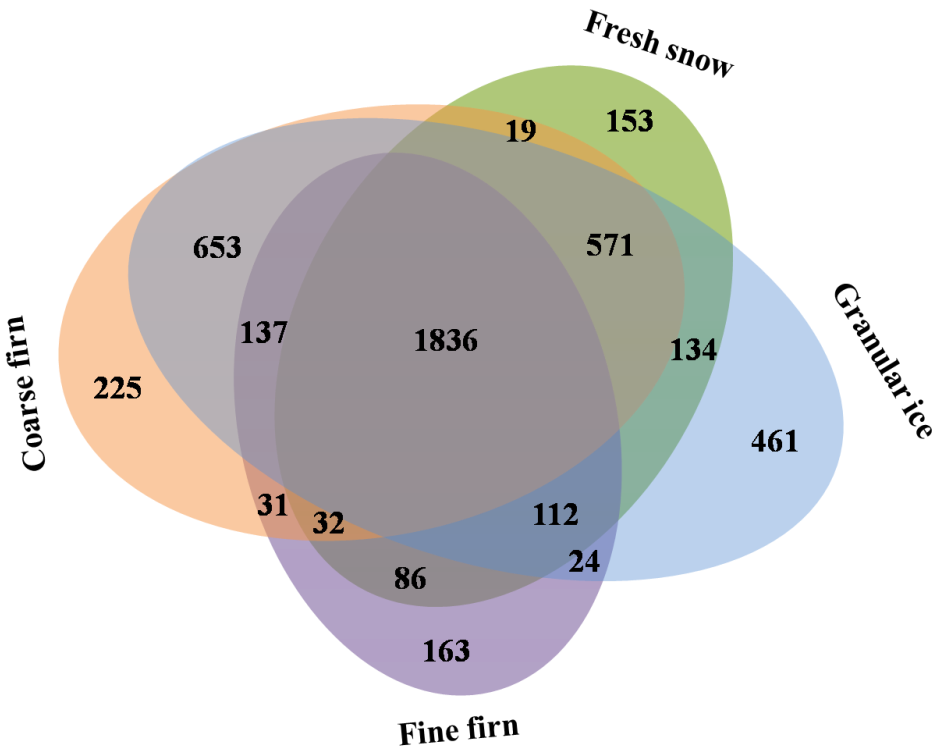

Figure 7. Four-way Venn diagram showing the overlap in molecular formulas between the fresh snow, fine firn, coarse firn and granular ice. The numbers within the diagram are the numbers of m/z molecular formulas that are unique to each type of sample.

Biogeosciences Discuss., https://doi.org/10.5194/bg-2017-507
Manuscript under review for journal Biogeosciences
Discussion started: 18 December 2017

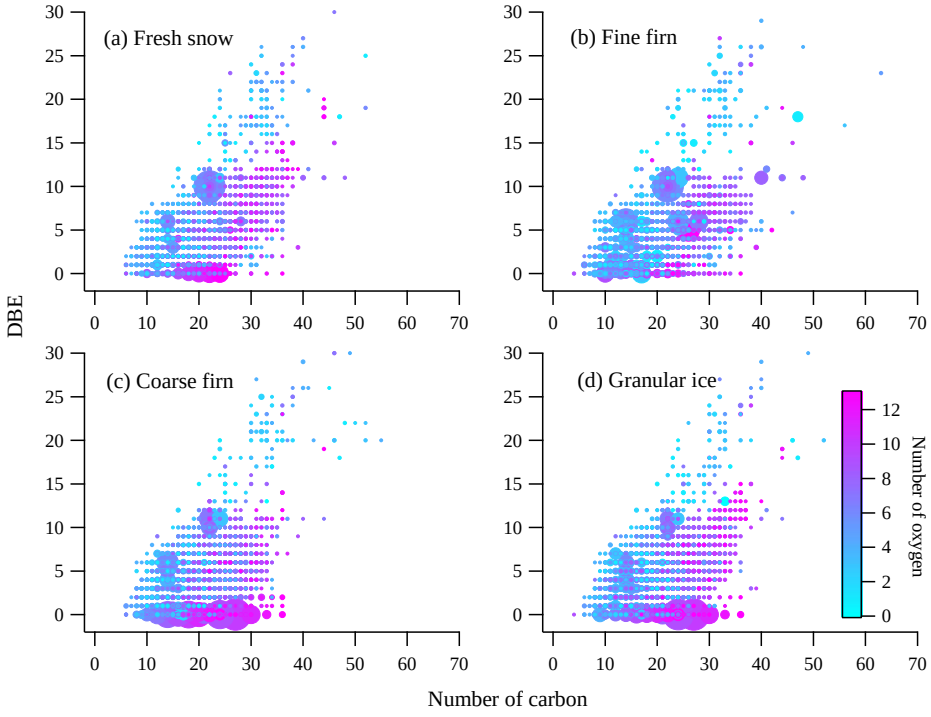

Figure 8.Iso-abundance plots of DBE versus carbon numbers for all DOM components, colored according to the number content of oxygen for(a) fresh snow, (b) fine firn, (c) coarse firn, and (d) granular ice.